

# Influence of Thermal Plasma Flow on the Daytime $F_2$ Layer

C. G. PARK

*Radioscience Laboratory, Stanford University, Stanford, California 94305*

P. M. BANKS

*Department of Applied Physics and Information Science, University of California at San Diego, La Jolla, California 92037*

The coupling between the daytime ionosphere and the overlying magnetosphere is investigated theoretically. Steady state plasma densities and fluxes are computed in the height range 150–3000 km from continuity and momentum equations for  $O^+$  and  $H^+$  ions. It is found that  $O^+$  densities near the  $F_2$  layer peak are remarkably insensitive to plasma densities in the overlying magnetosphere, in sharp contrast to the nighttime results reported earlier (Park and Banks, 1974). Plasma flow out of the daytime ionosphere increases with decreasing pressure in the magnetosphere, but the upward  $H^+$  flux reaches a well-known saturation limit before it can significantly reduce  $O^+$  densities in the  $F_2$  layer. Conversely, if the magnetospheric pressure is sufficiently high, plasma can flow downward into the sunlit ionosphere. However, in both cases the influence of such flows on ionospheric densities is not large owing to the dominating effect of photo-ionization within the  $F$  region. In the top side ionosphere it is found that  $H^+$  densities and the  $H^+-O^+$  transition height depend strongly on plasma densities in the overlying magnetosphere. It is concluded that the daytime plasmopause should be associated with the  $H^+$  trough in the top side ionosphere but not with the  $O^+$  trough within the  $F_2$  layer. In contrast, the nighttime plasmopause should produce a trough in both  $H^+$  and  $O^+$  densities. It is also concluded that plasma outflow cannot be responsible for depressions in  $N_m F_2$  observed in sunlit regions during ionospheric storms. However, it appears that changes in neutral gas composition or the  $O^+ + N_2$  reaction rate can easily account for such depressions.

## INTRODUCTION

In a recent paper [Park and Banks, 1974] we discussed theoretical models of thermal plasma flow between the ionosphere and the plasmasphere on the night side of the earth, where photo-ionization is almost completely absent. It was shown that in middle latitudes the plasmasphere acts as a large-capacity reservoir of thermal plasma and has a strong stabilizing influence on the peak electron density of the underlying ionosphere. When there are changes in  $F_2$  region conditions, plasma flow from the plasmasphere compensates for the changes such that the peak density of the  $F_2$  layer ( $N_m F_2$ ) remains nearly constant. It was also shown [Park and Banks, 1974] that  $N_m F_2$  depends strongly on the  $H^+$  density in the overlying plasmasphere and, consequently, on the abundance of neutral atomic hydrogen.

In this paper our previous work is continued by using theoretical models to investigate ionosphere-magnetosphere coupling in the day side ionosphere. The results show several important differences in the way sunlit and dark ionospheres are affected by the conditions in the overlying magnetosphere. The present results appear to agree with a number of recent observations of plasma flow between the ionosphere and the magnetosphere [Banks and Douppnik, 1974; Park, 1974], with the formation of light ion troughs in the top side ionosphere [Taylor and Walsh, 1972], and the effects of changes in neutral composition associated with the negative phase of ionospheric storms [Pröls and von Zahn, 1974].

## THEORY

Figure 1 illustrates the geometry of a magnetic flux tube and the coordinate system used in this paper. As we did before [Park and Banks, 1974], we assume that  $O^+$  is the only ion present in region 1 (150–500 km), whereas a mixture of  $O^+$  and  $H^+$  ions exists in region 2 (500–3000 km). In this paper we do

not attempt to calculate the plasma density distribution above 3000 km.

Assuming low flow speed and steady state conditions, we adopt the necessary flow equations for  $O^+$  and  $H^+$  ions from Park and Banks [1974]. In region 1 we have

$$(1/A) \partial [n(O^+)wA] / \partial z = p - \beta n(O^+) \quad (1)$$

for the  $O^+$  continuity equation and

$$w = -D \left\{ \frac{\partial \ln n(O^+)}{\partial z} + \frac{\partial \ln T_p}{\partial z} + \frac{1}{H_p} \right\} + w_D \quad (2)$$

for the  $O^+$  momentum equation. The notation in (1) and (2) is as follows:

- $A$  area of the magnetic flux tube, inversely proportional to magnetic field strength;
- $n(O^+)$   $O^+$  density;
- $w$  ion transport velocity in the vertical ( $z$ ) direction;
- $p$   $O^+$  production rate;
- $\beta$   $O^+$  loss coefficient;
- $D$  effective ambipolar diffusion coefficient of  $O^+$  including the effect of magnetic dip angle;
- $T_p = T_e + T_i$ ;
- $H_p = kT_p/m_i g$ ;
- $w_D$  vertical drift velocity imposed by electric fields or neutral winds.

The  $O^+$  ion production is due to photo-ionization of atomic oxygen by solar EUV ( $\lambda < 910 \text{ \AA}$ ) radiation. The production rate  $p$  is given by  $p = I(O)n(O)$ , where  $n(O)$  is atomic oxygen density and  $I(O)$  is the photo-ionization rate coefficient, which depends on the flux of ionizing radiation as well as on the ionization cross section. The ionization cross section depends on the energy state of the  $O^+$  ion produced, but for the purpose of computing  $O^+$  densities we need to consider only  $O^+(^4S)$  [Banks and Kockarts, 1973, chapter 20]. With this as-

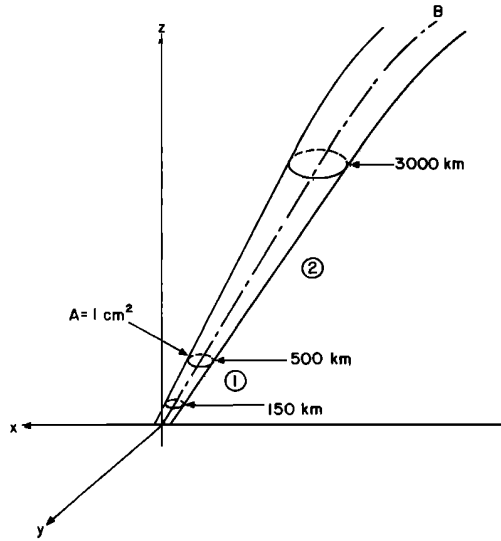


Fig. 1. Geometry of a flux tube with the two separate regions discussed in the text. The x axis points toward the north, and the y axis toward the west.

sumption we adopt a value  $I(O) = 3.3 \times 10^{-7} \text{ s}^{-1}$  for an overhead sun and low sunspot activity [Banks and Kockarts, 1973, chapter 6]. The values of the necessary rate coefficients have been given in Park and Banks [1974].

The vertical ion drift velocity  $w_D$ , measured positive upward, is given by

$$w_D = -(E_y/B) \cos I - U_x \sin I \cos I \quad (3)$$

where  $E_y$  is the westward component of the electric field,  $U_x$  is the northward component of neutral air wind, and  $I$  is the magnetic dip angle. Since we do not consider ion-air drag effects in this study, electric fields and neutral winds are equivalent in terms of the vertical drift that they impose on the plasma. The equivalence between  $E_y$ ,  $U_x$ , and  $w_D$  at 50° latitude is shown in Figure 2.

The O<sup>+</sup> density profile in region 1 can be found by using standard numerical techniques. For boundary conditions we specify a chemical equilibrium (i.e.,  $n = p/\beta$ ) at 150 km and a flux,  $\phi(O^+) = wn(O^+)$ , across the 500-km level. This flux boundary condition is an integral part of our calculations and is consistent with the fluxes present in region 2, as is discussed below.

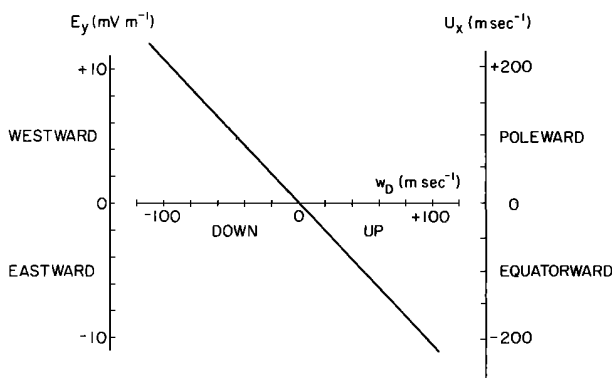


Fig. 2. Vertical ion drift velocity induced by an east-west component of the electric field or north-south neutral wind at 50° geomagnetic latitude and 300-km altitude.

For the thermal structure of region 1,  $T_e$  is taken from experimental results, and  $T_i$  is computed from  $T_e$  and  $T_n$  by using expressions given elsewhere [e.g., Banks and Kockarts, 1973, chapter 23].

In region 2, between 500 and 3000 km, steady state continuity and momentum equations for H<sup>+</sup> are written as

$$(1/A) \partial [n(H^+)w_1A]/\partial z = p_1 - \beta_1 n(H^+) \quad (4)$$

and

$$w_1 = -D_1 \left\{ \frac{\partial \ln [n(H^+)T_i]}{\partial z} + \frac{T_e}{T_i} \frac{\partial \ln (n_e T_e)}{\partial z} + \frac{1}{H_1} \right\} + w_D \quad (5)$$

where  $n_e$  is the electron density, the subscript 1 is used to refer to H<sup>+</sup> parameters, and the other symbols have the same meaning as they had before.

For O<sup>+</sup> in region 2 we assume that electrostatic equilibrium prevails, so that the momentum equation can be written as

$$\frac{\partial \ln [n(O^+)]}{\partial z} + \frac{T_e}{T_i} \frac{\partial \ln n_e}{\partial z} + \frac{\partial \ln T_i}{\partial z} + \frac{T_e}{T_i} \frac{\partial \ln T_e}{\partial z} + \frac{1}{H_2} = 0 \quad (6)$$

As was done in Park and Banks [1974], the H<sup>+</sup> density at 3000 km is specified as an arbitrary boundary condition which is varied to match various geophysical conditions. At 500 km, H<sup>+</sup> is assumed to be in chemical equilibrium with O<sup>+</sup> according to the relation

$$n_{500}(H^+) = \frac{9}{8} \left( \frac{T_n}{T_i} \right)^{1/2} \frac{n_{500}(O^+)n_{500}(H)}{n_{500}(O)}$$

With regard to O<sup>+</sup> in region 2 the 500-km boundary condition needed to solve (4), (5), and (6) is taken from the ion density computations of region 1, where O<sup>+</sup> is the dominant ion.

The electron temperature in region 2 is calculated by assuming a constant electron heat flux given by

$$F = -7.7 \times 10^5 T_e^{5/2} A \frac{\partial T_e}{\partial z} \text{ eV cm}^{-2} \text{ s}^{-1}$$

where  $F$  is the electron heat flux across the 500-km level and the other parameters are as defined previously. The ion temperature  $T_i$  is calculated from  $T_n$  and  $T_e$  in the same manner as was used for region 1.

With the above boundary conditions and parameters, self-consistent O<sup>+</sup> and H<sup>+</sup> densities are calculated from (4), (5), and (6) by the numerical procedures described in Park and Banks [1974].

### RESULTS

In this section we present results of computations of steady state H<sup>+</sup> and O<sup>+</sup> fluxes and densities obtained for daytime conditions at 50° invariant latitude. Neutral gas parameters have been taken from the 1000°K thermosphere tabulated by Banks and Kockarts [1973], while the electron temperature profile has been adopted from midday incoherent scatter radar measurements in July 1964 [Evans, 1967].

Results from a number of numerical computations of steady state plasma flow are summarized in Figure 3 in terms of the behavior of the H<sup>+</sup> and O<sup>+</sup> fluxes for various electric field strengths and H<sup>+</sup> upper boundary densities. In the steady state the number of O<sup>+</sup> ions passing along a magnetic flux tube

from region 1 to region 2 must be equal to the number of  $H^+$  ions passing through the upper (3000 km) boundary. Since the thermal plasma flow is confined to magnetic flux tubes, however, the  $H^+$  and  $O^+$  fluxes are not directly comparable unless they are normalized to some equivalent unit area. Here we adopt the method given in *Park and Banks* [1974] and normalize the  $O^+$  and  $H^+$  fluxes to an altitude of 500 km, adopting a magnetic flux tube area obtained through computation of magnetic field intensity. The solid curves in Figure 3 give the normalized  $H^+$  flux (a positive flux corresponds to outward flow) as a function of the  $O^+$  density at 500 km for four values of the overlying  $H^+$  density. For a given upper boundary density it can be seen that inward or outward  $H^+$  flows are possible, depending on the magnitude of the  $O^+$  density at 500 km. When the  $F_2$  region  $O^+$  density is low, an inward flux of ionization is induced from the plasma reservoir lying above 3000 km in sufficient magnitude to help sustain the ionosphere. Likewise, for a fixed ionospheric density at 500 km, decreases in the 3000-km  $H^+$  boundary density lead to progressively greater ionization outflows from the ionosphere which eventually saturate at the limiting flux [Geisler, 1967; Banks and Holzer, 1969].

The set of dashed curves in Figure 3 gives the 500-km  $O^+$  flux as a function of the 500-km  $O^+$  density for five values of the applied electric field. (For convenience, vertical drift effects are shown in terms of  $E_y$ . See Figure 2 for equivalent  $U_x$  and  $w_D$ .) In the steady state, continuity of plasma flux in regions 1 and 2 requires that the normalized  $H^+$  flux at 3000 km equal the  $O^+$  flux at 500 km. Consequently, any intersection between a solid curve and a dashed curve represents a possible steady state solution involving the plasma flux, the applied electric field, the 500-km  $O^+$  density, and the 3000-km  $H^+$  density. For normal daytime conditions when the electric field is small, the steady state solution lies in the upper half of the figure, corresponding to plasma flow from the ionosphere into the magnetosphere. This upward flow replenishes the magnetospheric regions which have been partially depleted at night through downward flow into the ionosphere [Park, 1974].

To show the influence of thermal plasma flow upon the  $F_2$  layer peak density, Figure 4 gives information similar to that of Figure 3 except that now the horizontal axis represents the  $F_2$  layer peak density  $N_m F_2$ . It is immediately clear that for a given value of electric field  $E_y$ ,  $N_m F_2$  is relatively insensitive to the plasma density at 3000 km. On the other hand,  $N_m F_2$  is significantly affected by electric fields (or neutral winds), particularly if the imposed drift is upward. These results are well known [e.g., Hanson and Patterson, 1964; Schunk and Walker, 1970, 1973] and contrast sharply with the nighttime behavior reported in *Park and Banks* [1974]. In the case of a nocturnal  $F_2$  layer, maintained primarily by downward flow of plasma from the overlying magnetosphere,  $N_m F_2$  is strongly controlled by the plasma pressure in the magnetosphere. Vertical drift has little effect on the  $N_m F_2$  at night because changes in recombination loss rates resulting from vertical displacement of the layer tend to be compensated by simultaneous adjustments in downward flux. In a sunlit ionosphere the dominant ionization source is photo-ionization of neutral oxygen atoms, and plasma flow into or out of the magnetosphere has relatively little effect on  $N_m F_2$ . These day and night differences are further illustrated in Figures 5–7.

In Figure 5,  $O^+$  (solid curves) and  $H^+$  (dashed curves) density profiles are shown for three different assumed values of  $n_{3000}(H^+)$ . Other assumptions include an overhead sun and no

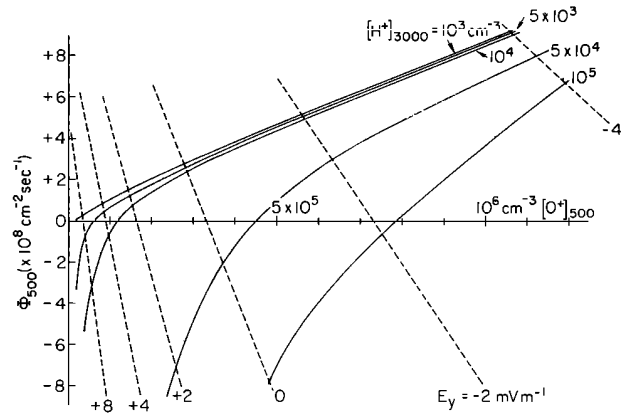


Fig. 3. Results for plasma flux as a function of the 500-km  $O^+$  density. The solid curve shows the  $H^+$  flux at 3000 km (normalized by flux tube area to 500 km) as a function of the 500-km  $O^+$  density. The dashed lines give the 500-km  $O^+$  flux for different values of  $E_y$ .

vertical drift. Case 1, with  $n_{3000}(H^+) = 10^3 \text{ cm}^{-3}$ , approaches the limiting flux condition, and  $H^+$  remains a minor ion up to 3000-km altitude. In case 2,  $H^+$  densities are much higher at all altitudes, and the  $H^+-O^+$  transition level is lowered to about 1500 km, although the upward flux remains close to the limiting value. Case 3 represents a situation where the  $H^+$  density at 3000 km is sufficiently large to cause the plasma to flow downward into the ionosphere. It is evident that the 3000-km  $H^+$  density has remarkably little effect on the  $O^+$  distribution, particularly near the  $F_2$  layer peak. We also note that the changes in the  $O^+$  scale height above 1000 km are due to changes in the charge separation electric field, which depends on the plasma composition.

To compare these results with the nighttime behavior, the calculations have been repeated with the photo-ionization term set to zero and electron temperature data for midnight in November 1964 used [Evans, 1967]. These nighttime results are shown in Figure 6. Unlike the daytime case, the  $H^+$  density at 3000 km during the night has a strong influence on the  $O^+$  density profile at all altitudes. In addition, the  $H^+-O^+$  transition level remains about the same for large changes in the 3000-km  $H^+$  density. Figure 7 shows the dependence of  $N_m F_2$  on  $n_{3000}(H^+)$  for the daytime and nighttime conditions il-

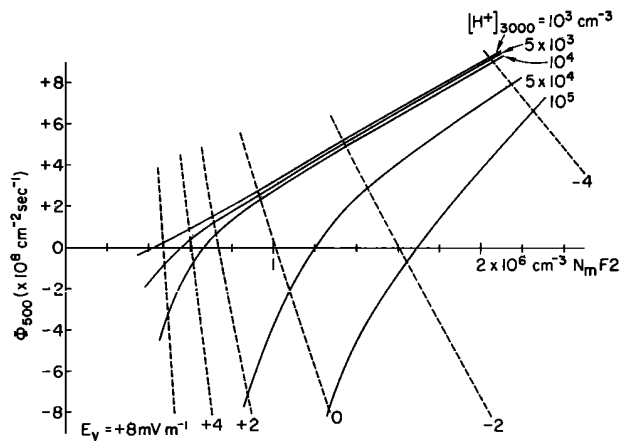


Fig. 4. Results for plasma flux as a function of the  $F_2$  layer peak density  $N_m F_2$ . The solid curves give the  $H^+$  flux at 3000 km (normalized to 500 km) as a function of  $N_m F_2$ , while the dashed curves give the  $O^+$  flux for different values of  $E_y$ .

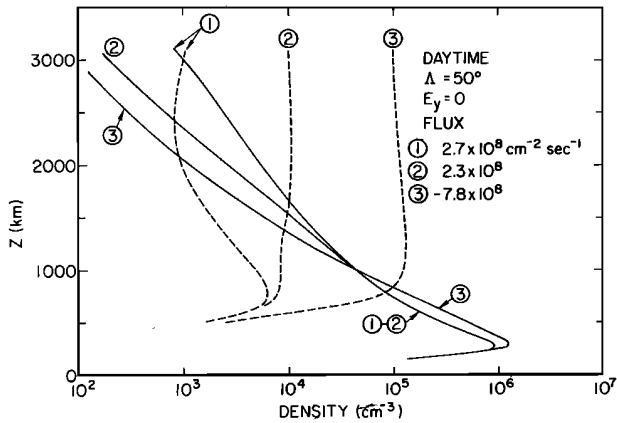


Fig. 5. Examples of daytime  $O^+$  (solid curves) and  $H^+$  (dashed curves) density profiles for three different values of the 3000-km  $H^+$  density.

illustrated in Figures 5 and 6, respectively. At night,  $N_m F_2$  is almost directly proportional to  $n_{3000}(H^+)$ , whereas in the daytime,  $N_m F_2$  remains nearly constant as  $n_{3000}(H^+)$  changes by a factor of 1000.

DISCUSSION

The results given in the last section have important implications for our understanding of plasmasphere-ionosphere coupling processes and the formation of the ionospheric trough. On the night side of the earth the simple model described here and in *Park and Banks* [1974] predicts that the large  $H^+$  density drop across the plasmapause should produce a corresponding density decrease in the underlying  $F_2$  layer. On the day side, however, the abrupt change in high-altitude thermal plasma density which occurs at the plasmapause does not greatly affect the  $F_2$  layer. Thus we conclude that on the day side of the earth the high-altitude plasmapause should occur near the equatorward edge of the light ion trough seen in the top side ionosphere [Taylor and Walsh, 1972]. The  $O^+$  depletion characteristic of the mid-latitude electron density trough seen in the  $F_2$  layer and below, however, does not result from outward plasma flow and is not directly related to the plasmapause. Such a conclusion follows directly from the results given in Figure 5. In addition, analyses of satellite and radio whistler data [Banks and Doupnik, 1973; Park, 1974] sup-

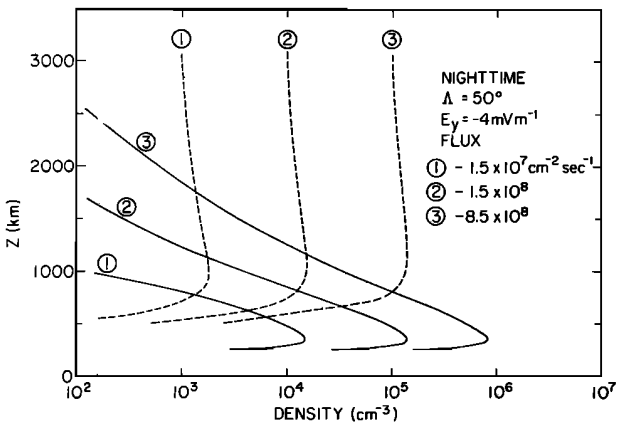


Fig. 6. Examples of nighttime  $O^+$  (solid curves) and  $H^+$  (dashed curves) density profiles for three different values of the 3000-km  $H^+$  density.

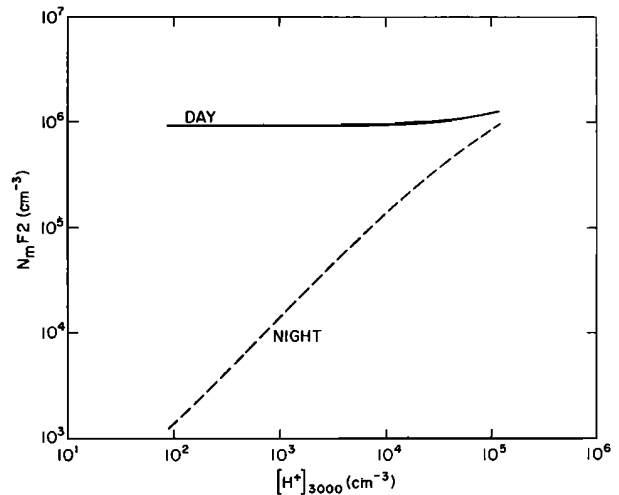


Fig. 7. Dependence of  $N_m F_2$  on the 3000-km  $H^+$  density for day and night.

port the idea that the sunlit ionosphere can supply a large flux of plasma to the magnetosphere without creating significant depression in  $N_m F_2$ .

During the negative phase of ionospheric storms, large decreases occur in  $N_m F_2$ . The results given here indicate that such depressions, on the day side, are not caused by plasma flowing from the ionosphere into the plasma-depleted magnetosphere. On the other hand, there is strong evidence that the storm negative phase is associated with changes in the neutral atmosphere composition. *Pröls and von Zahn* [1974], for example, reported recent Esro 4 satellite observations during and following a magnetic storm where enhanced  $N_2$  densities were found to coincide with a region of decreased  $N_m F_2$ . The effects of such neutral composition changes on the ionosphere have been calculated here by using the previously described model. The results are shown in Figures 8 and 9.

Figure 8 uses the same format as is used in Figure 5, the solid curve showing  $H^+$  flux as a function of  $n_{500}(O^+)$ . For reference, two dashed curves are taken from Figure 5 to give the  $O^+$  flux as a function of  $n_{500}(O^+)$ . The solid-dashed lines show the effect of increasing the  $N_2$  density by a factor of 5: the

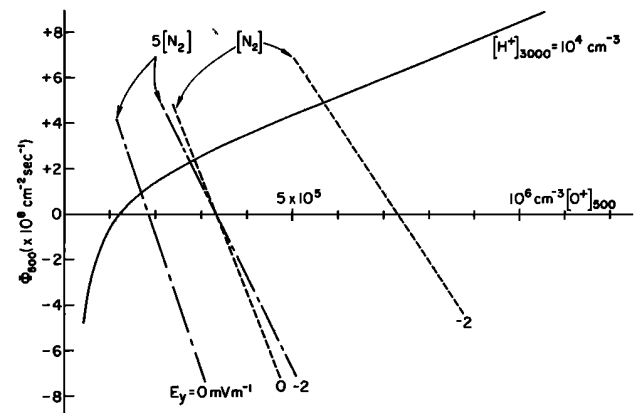


Fig. 8. Effects of an increase in the  $N_2$  density. The solid curve gives the  $H^+$  flux at 3000 km (normalized to 500 km) as a function of the  $O^+$  density at 500 km. The dashed lines, taken from Figure 3, give the  $O^+$  flux at 500 km for an undisturbed thermosphere, while the solid-dashed lines give the  $O^+$  flux when the  $N_2$  density is increased at all altitudes by a factor of 5.

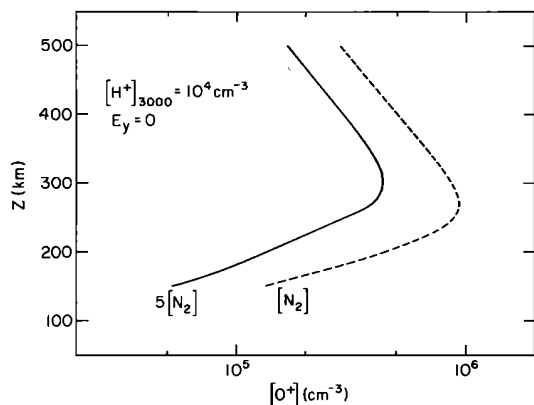


Fig. 9. Effects of a fivefold increase in the  $N_2$  density on the  $O^+$  density profile in the  $F$  region.

steady state flux into the magnetosphere and the 500-km  $O^+$  density are reduced by a factor of 2. Figure 9 shows the effects on the  $O^+$  density profile below 500 km. A fivefold increase in the  $N_2$  density reduces  $N_m F_2$  by a factor of  $\sim 2$  and at the same time raises the height of the peak,  $h_m F_2$ , by  $\sim 30$  km. These results are in good agreement with observations and also with previous theoretical work [e.g., King, 1971; Duncan, 1969; Chandra and Herman, 1969; Chandra and Stübbe, 1971].

The overall problem of a disturbed ionosphere is somewhat more complex than that described above, however, owing to the presence of  $NO^+$ . As the  $O^+$  density in the  $F$  region declines as a consequence of the increasingly rapid reaction  $O^+ + N_2 \rightarrow NO^+ + N$ ,  $NO^+$  will increase in density subject to its own loss process of dissociative recombination. Both electric field induced ion drift and enhanced  $N_2$  densities affect the  $O^+ + N_2$  reaction rate [Banks et al., 1974; Schunk et al., 1975]. As a consequence, daytime electron density troughs and the larger regions of ionospheric storm depletion may involve  $NO^+$  as an important ion in the  $F_2$  layer [e.g., Taylor et al., 1975].

#### CONCLUSIONS

The present theoretical study emphasizes the differences in the way that the daytime and nighttime  $F_2$  layers are affected by the thermal plasma density in the overlying magnetosphere. At night the magnetosphere acts as a replenishing plasma reservoir for the  $F_2$  layer and therefore has a strong influence on the ionospheric densities. In the daytime,  $O^+$  ions in the  $F_2$  layer are copiously produced by photo-ionization, and fluxes into or out of the magnetosphere have little effect on  $O^+$  densities. These fluxes, however, have large effects on  $H^+$  densities in the top side ionosphere. We conclude from these results that the daytime plasmopause should be associated with the  $H^+$  trough in the top side ionosphere but not with the trough in  $O^+$  density or  $N_m F_2$ . At night the plasmopause

can be identified with a trough in both  $H^+$  and  $O^+$  densities. Finally, daytime ionospheric depletions associated with geomagnetic disturbances are likely to arise from enhanced  $O^+ + N_2$  reactions associated with a greater reaction rate (ion drift effect) or enhanced  $N_2$  densities.

*Acknowledgments.* We wish to thank R. W. Schunk, J. R. Doupnik, W. J. Raitt, and H. Rishbeth for many helpful discussions. This research was sponsored in part under National Science Foundation grant GA-28042 at Stanford University and by the National Aeronautics and Space Administration under grants NGR-05-009-075 and NSG-7001 at the University of California at San Diego.

The Editor thanks P. Stubbe and J. C. G. Walker for their assistance in evaluating this paper.

#### REFERENCES

- Banks, P. M., and J. R. Doupnik, Thermal proton flow in the plasmasphere: The morning sector, *Planet. Space Sci.*, **22**, 79, 1974.
- Banks, P. M., and T. E. Holzer, Features of plasma transport in the upper atmosphere, *J. Geophys. Res.*, **74**, 6304, 1969.
- Banks, P. M., and G. Kockarts, *Aeronomy*, Academic, New York, 1973.
- Banks, P. M., R. W. Schunk, and W. J. Raitt,  $NO^+$  and  $O^+$  in the high-latitude  $F$  region, *Geophys. Res. Lett.*, **1**, 239, 1974.
- Chandra, S., and J. R. Herman,  $F$  region ionization and heating during magnetic storms, *Planet. Space Sci.*, **17**, 841, 1969.
- Chandra, S., and P. Stubbe, Ion and neutral composition changes in the thermospheric region during magnetic storms, *Planet. Space Sci.*, **19**, 491, 1971.
- Duncan, R. A.,  $F$ -region seasonal and magnetic-storm behavior, *J. Atmos. Terr. Phys.*, **31**, 59, 1969.
- Evans, J. V., Mid-latitude  $F$ -region densities and temperatures at sunspot minimum, *Planet. Space Sci.*, **15**, 1389, 1967.
- Geisler, J. E., On the limiting daytime flux of ionization into the protonosphere, *J. Geophys. Res.*, **72**, 81, 1967.
- Hanson, W. B., and T. N. L. Patterson, The maintenance of the nighttime  $F$  layer, *Planet. Space Sci.*, **12**, 979, 1964.
- King, G. A. M., The ionospheric  $F$ -region storm, *J. Atmos. Terr. Phys.*, **33**, 1223, 1971.
- Park, C. G., Some features of plasma distribution in the plasmasphere deduced from antarctic whistlers, *J. Geophys. Res.*, **79**, 169, 1974.
- Park, C. G., and P. M. Banks, Influence of thermal plasma flow on the mid-latitude nighttime  $F_2$  layer: Effects of electric fields and neutral winds inside the plasmasphere, *J. Geophys. Res.*, **79**, 4661, 1974.
- Prölls, G. W., and U. von Zahn, Esro 4 gas analyzer results, 2, Direct measurement of changes in the neutral composition during an ionospheric storm, *J. Geophys. Res.*, **79**, 2535, 1974.
- Schunk, R. W., and J. C. G. Walker, Minor ion diffusion in the  $F_2$ -region of the ionosphere, *Planet. Space Sci.*, **18**, 1319, 1970.
- Schunk, R. W., and J. C. G. Walker, Theoretical ion densities in the lower ionosphere, *Planet. Space Sci.*, **21**, 1875, 1973.
- Schunk, R. W., W. J. Raitt, and P. M. Banks, Effect of electric fields on the daytime high latitude  $E$  and  $F$  regions, *J. Geophys. Res.*, **80**, in press, 1975.
- Taylor, H. A., Jr., and W. J. Walsh, The light ion trough, the main trough, and the plasmopause, *J. Geophys. Res.*, **77**, 6716, 1972.
- Taylor, H. A., Jr., J. M. Grebowsky, and A. J. Chen, Ion composition irregularities and ionosphere-plasmasphere coupling: Observations of a high latitude ion trough, submitted to *J. Atmos. Terr. Phys.*, 1975.

(Received November 8, 1974;  
revised February 7, 1975;  
accepted February 25, 1975.)